DOI: 10.13009/EUCASS2019-683

Plasma actuation for lifted flame stabilization in coaxial methane-air flow

Maria Grazia De Giorgi, Antonio Ficarella*, Donato Fontanarosa*, Elisa Pescini* and Antonio Suma**
**Dept. of Engineering for Innovation, University of Salento, Via per Monteroni "Campus Ecotekne", LECCE I-73100, Italy*

Abstract

The flame stabilization represents a relevant issue in aero-engine design. In fact, the growing demand of pollutant emissions reduction without significant losses of the combustion efficiency has driven the efforts of the scientific community towards lean flames. Lean fuel mixtures, characterized by low temperature flames, could manifest an unstable behaviour which can easily lead to the flame extinction due to the establishment of the blowout condition. This requires the implementation of control systems to avoid flame instability occurrence.

The present work shows an investigation of the impact of dielectric barrier discharge (DBD) plasma actuation on lifted flame stabilization in a methane CH_4-air Bunsen burner at ambient conditions.

Two different plasma actuator configurations, powered with a high voltage (HV)/high frequency sinusoidal signal, have been investigated. Once the best actuator configuration was selected, the efficiency of the plasma actuation has been evaluated in terms of the flame lift-off distance, length and shape. In particular, in order to change the actuator power dissipation, different peak-to-peak voltages V_{pp} were tested, while the actuation frequency was kept equal to 20 kHz. The application of plasma discharges to flame stabilization leads to plasma-attached flames or plasma-enhanced lifted flames, depending on the air and fuel flow rates. At air flow rate of 1.54 g/s, plasma actuation allowed to decrease the lift-off height until the fuel jet velocity was below about 0.05 m/s thanks to the extension of the flame region upstream, toward the burner exit section. Beyond this value, it had no significant impact on the flame lift-off height, even though the amplitude of the lift-off height oscillations reduced coupled with a more stable behaviour of the lifting flame. The benefit of the plasma actuation increased by reducing the air flow rate to 1.35 g/s. In this condition, plasma-assisted flame reattachment was evident at each fuel velocity, in combination with an increasing flame height proportionally to the fuel jet velocity.

1. Introduction

A typical issue in aero-engine design is the reduction of NOx emissions without relevant losses of the combustion efficiency.

To this aim, low temperature flames of lean fuel mixture is a promising solution [1][2]. However, lean flames could manifest an unstable behaviour that can easily bring to unsteady effects and flame quenching as leaner conditions are approached. Flame blow-off is usually anticipated by the lifting of the flame. To avoid blow off of premixed or partially premixed flames the use of pilot flames is often used [3]. Non-premixed diffusive flames manifest a better stability under wide ranges of operating conditions and safety [1] [4].

The stabilization of turbulent non-premixed flames has been studied in [5]. The stability of lifted diffusion jet flame is influenced by local flame extinction, in the flame area where the outer mixing layer merges with the central flame front [6]. The stabilization of the edge flame for non-premixed flames propagating in laminar and turbulent flows was also affected by the velocity gradient and the burnt gas expansion on edge flame propagation [7]propagation. Furthermore Fokaides et al. [8] experimentally characterized the flow pattern, the mixing evolution and the temperature distribution of a lifted-stabilized swirl flame near its lean blowout.

In literature, several techniques have been investigated to avoid the flame instability. Flame control systems are mainly passive, as the modification of the air injection geometry such as swirlers and flame holders, in order to obtain flame stability by to the establishment of large-scale vortexes. These flow structures permits a turbulent mixing and hot gases recirculation and extend the mixture flammability range. Furthermore, active flow control devices can also be adopted, which allow adjustment of control parameters according to real-time operation conditions. Among them, a very promising technique is based on the use of plasma, due to their high flexibility and extremely short response time.

DOI: 10.13009/EUCASS2019-683

Previous studies have shown that plasmas and electric field can positively affect combustion, in particular by the stabilization of ultra-lean flames, decrease of ignition delay time, extension of flammability limits and increase of the burning velocity.
Plasma discharges produce combined effects which impact on thermal, kinetic and transport mechanisms [9, 10]. Combustion is improved by the local production of new radicals and ionized species as well as by momentum and turbulence promotion by the motion of the electric carriers due to the electric field. Recent studies investigated the flame stabilization by using non-thermal plasma (NTPs) electrical discharges, sometimes called non-equilibrium or 'cold 'plasmas. Non-thermal plasmas manifest high energy efficiency, due to low ionization/excitation energy with respect to the total energy consumption, and low increase in temperature. Characteristic electron temperatures in plasma discharges are of few electron volts, which permit to dissociate the fuel and to produce free radicals [11, 12]. High voltage (HV) discharges have been also investigated with the aim to improve the fuel/air mixtures ignition [13, 14], to increase flame propagation [15, 16], to enhance flame stabilization [17, 18, 19, 20, 21], and to extend flammability limits [22].
A promising non-thermal plasma device is the DBD, also called silent discharge. Non-equilibrium DBD plasmas can be produced between two electrodes on the dielectric surface when an alternating current (AC) HV passes through them [23, 24, 25, 26, 27].
In the present work, the effect of a sinusoidal plasma actuation on the flame lift-off distance, length and shape has been experimentally investigated in a Bunsen-type burner with an inner CH_4 jet surrounded by an outer air jet. First, plasma actuator configuration which had the highest control authority was chosen. Then, lift-off experiments in both absence and presence of plasma actuation were performed.

2. Experimental setup, methods and methodologies

The experimental setup consisted of: a coaxial Bunsen burner equipped with a plasma actuator, two gas feeders equipped with flow meters, a HV generator, a HV probe and a current transformer for the electrical power measurements (FIGURE 1).

The Bunsen burner was composed two coaxial quartz tubes. The inner one had an external diameter of 10 mm, a thickness was 1 mm and was fed by CH_4. The coaxial outer tube had an external diameter of about 30 mm, a thickness of 2 mm and was fed by air. The coaxial flow configuration was then a typical normal diffusive flame (NDF). The top ends of the two coaxial tubes were aligned as shown in FIGURE 1, thus there was no mixing zone inside the quartz tube and the flame ignition occurred at the exit of the quartz tubes.

The air flow rate was measured with accuracy of ±3% of reading ± 0.3% full-scale, while the CH_4 injection was measured with accuracy of ±0.8% of reading ±0.2% full-scale.

The non-thermal plasma generation system involved a DBD reactor and a power supply. The former consisted of an internal copper needle having a diameter of 1 mm and connected to the ground (herein referred as grounded electrode), coupled with a copper corona of 30 mm length, 1 mm thickness and 30 mm inner diameter. The corona was rolled up on the outer surface of the outer quartz tube, fastened to it by screws and connected to the HV (herein referred as HV electrode). A sinusoidal high frequency, HV signal produced by an HV generator (the PVM500 Plasma Resonant and Dielectric Barrier Corona Driver, commercialized by Information Unlimited®) powered the HV electrode, while the other electrode was connected to ground.

The standoff distance, S_{SO}, which is the distance between the upper lip of the plasma grounded electrode and the mixing region, was set to -40 mm and 20 mm. Therefore, the plasma actuation affected both the fuel/air activation and the fuel-air mixing.
The applied voltage $V(t)$ was acquired by using the HV probe Tektronix P6015A, with a measurement accuracy of ±3%. Different V_{pp} voltages were tested at fixed actuation frequency equal to 20 kHz. The current flowing in the circuit $I(t)$ was measured through a current transformer Bergoz mod. CT-C1.0-BNC with accuracy of ±0.5%. Both the HV probe and the current transformer were connected to the oscilloscope (Tektronix TDS2024C) and the respective signals were recorded simultaneously with an accuracy of $\pm$ 3%. The acquisition sample rate was set to 25 MHz and each measurement point was given by the average of 128 acquisition. Measured data were used for determining the electrical power dissipation.
The electrical power consumption of the DBD was calculated by:

$$P_{el} = \frac{1}{T}\int_0^T I(t) \cdot V(t) \cdot dt; \quad (1)$$

where T is the period of the applied voltage.

In order to characterize the impact of the plasma actuation, the visible flame appearance was captured using a camera Canon EOS 700D camera, equipped with a Canon EFS 55-250mm lens, and a high-speed camera (Memrecam GX-1F), equipped with Sigma Macro lens 105mm. Regarding the high-speed camera, for each test

DOI: 10.13009/EUCASS2019-683

condition 500 single-images (resolution of 348 pixels x 480 pixels) have been captured at an acquisition rate of 500 Hz.

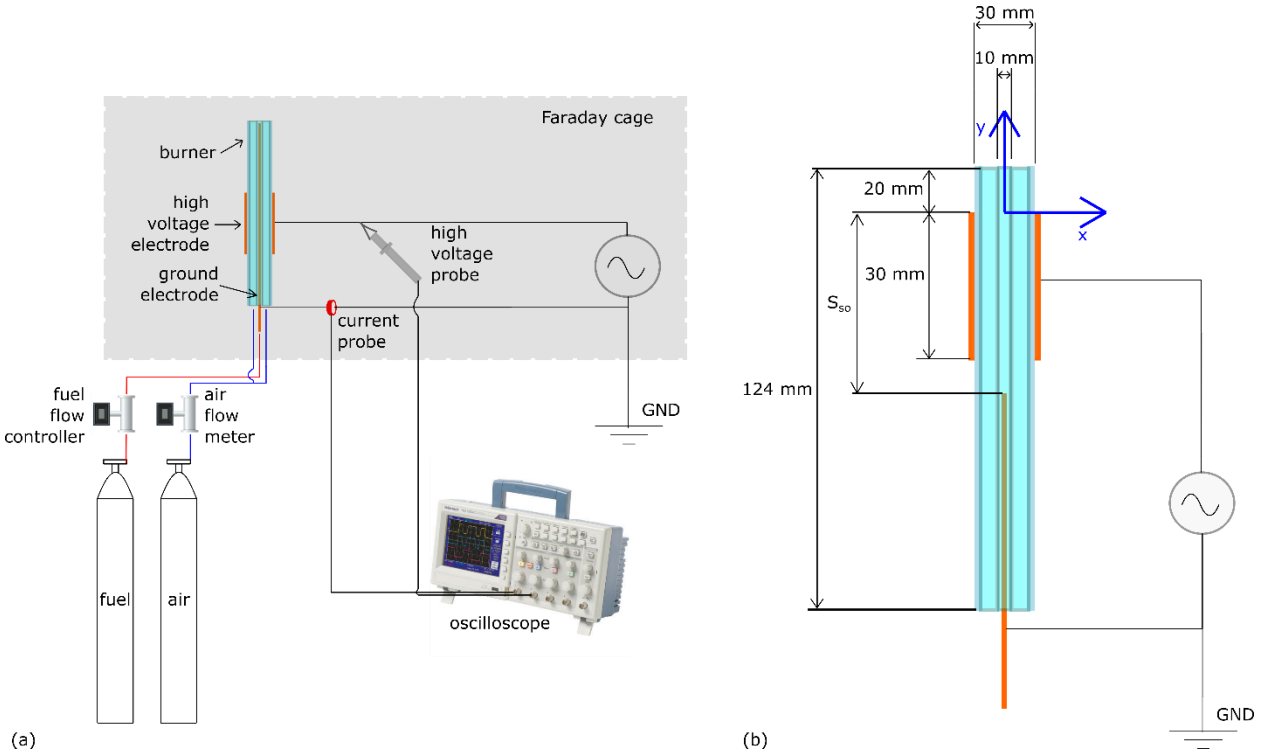

FIGURE 1. Experimental setup: (a) general schematic; (b) Sketch of the burner geometry together with the plasma actuator and reference system.

3. Test cases

Six different experimental campaigns were performed. The first run aimed to determine the effect of the standoff distance on the flame lift-off, at fixed air and fuel mass flow rates. Test cases 1b and 1c were performed at similar V_{pp}, but different standoff distances. In particular, two plasma actuator configurations have been tested, characterized by a different standoff distance, namely S_{SO}=-40 mm (see FIGURE 2 on the left) and S_{SO}=20 mm (see FIGURE 2 on the right). The flame behavior in presence of actuation was analyzed and compared with the one in absence of actuation (test case 1a). It was verified that the standoff distance had a negligible effect on the lift off condition in absence of actuation, therefore the configuration with S_{SO}=-40 mm was considered for further comparisons. The V_{pp} voltage was gradually increased in test cases 1d and 1e, in order to augment the plasma control authority, as it will be demonstrated in the next section.

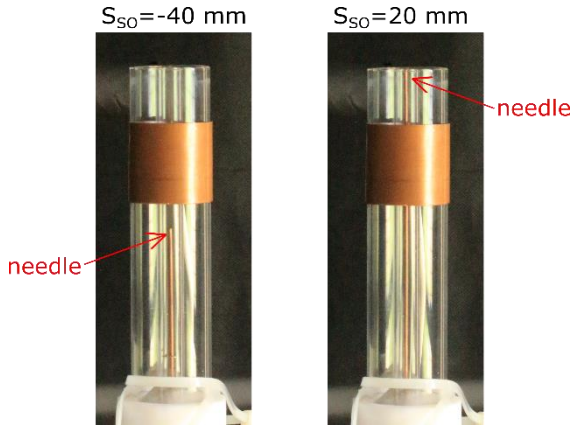

FIGURE 2. Plasma actuator DBD configurations: S_{SO}=-40 mm on the left and S_{SO}=20 mm on the right.

DOI: 10.13009/EUCASS2019-683

The second and third campaigns of experiments were carried out at fixed air flow rate, fixed S_{SO} (chosen on the base of the results of the first campaign) and increasing fuel flow rate. The run 3 was in absence of actuation, while the run 4 was characterized by the same fuel and air flow rates tested in the run 3, but in presence of actuation (at fixed V_{pp} voltage and frequency). In the run 4-5-6, the air flow rate was lowered and different plasma actuation dissipated powers (obtained by changing the applied V_{pp} voltages) were tested.

TABLE 1 shows the final test matrix of the entire set of experiments. The fuel-to-air equivalence ratio Φ was defined as $\Phi = (\dot{m}_f/\dot{m}_a)/(\dot{m}_f/\dot{m}_a)_{st}$, where $\dot{m}$ is the mass flow rate and the subscripts f, a and st denote the fuel, the air and the stoichiometric conditions respectively. A value of 17.19 was assumed for $(\dot{m}_a/\dot{m}_f)_{st}$. For the combustion power Q_b calculation, the CH_4 lower heating value was chosen equal to 50 MJ/kg.

TABLE 1 Test matrix of experiments and operating conditions. Plasma actuation frequency of 20 kHz.

	Test case	**S_{SO} [mm]**	**$\dot{m}_a$ [g/s]**	**$\dot{m}_f$ [g/s]**	**Φ [-]**	**V_{pp} [kV]**	**P_{el} [W]**	**Q_b [W]**
Run 1	1a	-40	1.11±0.02	0.0023±0.00009	0.035±0.009	0	0	112±5
	1b	-40				10.6±0.4	0.049±0.003	
	1c	20				11.1±0.5	0.27±0.02	
	1d	20				15.2±0.6	0.47±0.03	
	1e	20				18.4±0.8	1.13±0.06	
Run 2	2a	-40	1.54±0.03	0.0005±0.0001	0.006±0.001	0	0	27±5
	2b			0.0011±0.0001	0.012±0.001			55±5
	2c			0.0016±0.0001	0.018±0.001			82±5
	2d			0.0027±0.0001	0.031±0.001			137 ±5
	2e			0.0055±0.0002	0.061±0.003			270±10
Run 3	3a	-40	1.54±0.03	0.0005±0.0001	0.006±0.001	10.7±0.3	0.071±0.002	27±5
	3b			0.0011±0.0001	0.012±0.001			55±5
	3c			0.0016±0.0001	0.018±0.001			82±5
	3d			0.0027±0.0001	0.031±0.001			137 ±5
	3e			0.0055±0.0002	0.061±0.003			270±10
Run 4	4a	-40	1.35±0.03	0.0011±0.0001	0.014±0.001	0	0	55±5
	4b			0.0033±0.0001	0.042±0.002			164 ±5
	4c			0.0055±0.0002	0.070±0.003			270±10
Run 5	5a	-40	1.35±0.03	0.0011±0.0001	0.014±0.001	10.5±0.3	0.073±0.003	55±5
	5b			0.0033±0.0001	0.042±0.002			164 ±5
	5c			0.0055±0.0002	0.070±0.003			270±10
Run 6	6a	-40	1.35±0.03	0.0011±0.0001	0.014±0.001	16.2±0.4	0.26±0.01	55±5
	6b			0.0033±0.0001	0.042±0.002			164 ±5
	6c			0.0055±0.0002	0.070±0.003			270±10

4. Flame imaging results

The figures below show the effect of the standoff distance on the flame anchoring. As is it evident from FIGURE (a), at peak-to-peak voltage of about 11 kV, the flame reattached to the lips of the inner quartz tube when S_{SO} =-40 mm (test case 1b). This did not happen in the configuration with a S_{SO} =20 mm (test case 1c) which did not reattach the flame, showing no differences with the clean case. In addition, the dissipated power with S_{SO} =-40 mm was around 18% lower than the one measured at S_{SO} =20 mm. When using the actuator configuration with S_{SO} =20 mm, a partially reattached flame condition was observed by increasing V_{pp} to 15.2 kV (test case 1d), and the complete reattachment occurred only when the peak-to-peak voltage was 18.4 kV (test case 1e). In order to reattach the flame in the configuration with S_{SO} =20 mm, a power consumption equal to 23 times the one retrieved with S_{SO} =-40 mm was needed, as shown in FIGURE (b).

DOI: 10.13009/EUCASS2019-683

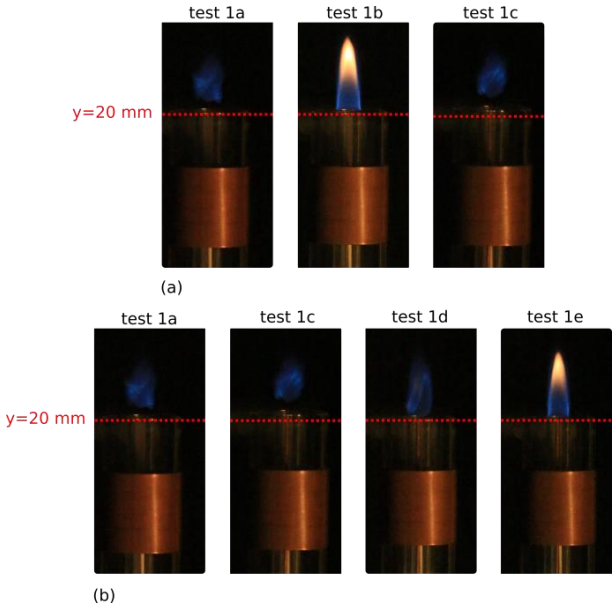

FIGURE 3. Modification of the flame appearance due to plasma actuation under lift-off condition: (a) impact of the stand-off (test 1b at S_{SO}=-40 mm, test 1c S_{SO}=20 mm) at fixed peak-to-peak voltage in comparison with the clean case (test 1a); (b) flame reattachment behavior by increasing the supplied peak-to-peak voltage for S_{SO}=20 mm.

From results was evident that S_{SO} =-40 mm had higher performance, therefore that standoff distance was used for further investigations.

As it is reported in FIGURE 4, at an air flow rate equal to 1.54±0.03 g/s the plasma discharge has an impact on the average flame lift-off height. The plasma actuation becomes less effective on lowering lift-off height when the fuel flow rate is increased. The application of plasma discharges to decrease the lift-off height is effective until the fuel jet velocity reaches 0.05 m/s. Beyond this value, the plasma has no significant impact on the flame lift-off height, as confirmed by the flame imaging shown in FIGURE 5. In fact, with respect to the clean configuration involving the cases of the experimental run 2, the presence of the plasma actuation extended the flame region toward the burner exit section for fuel jet velocities lower than 0.05 m/s (test cases 3a, 3b and 3c). At higher fuel jet velocity (test case 3d and 3e), this effect weakened even though the amplitude of the lift-off height oscillations reduced with respect to the clean case, and the lifting flame behavior became more stable.

The benefit of the plasma actuation improves by reducing the air flow rate. In particular, when fixing the air flow rate to 1.35±0.03 g/s while keeping constant the fuel flow rate, the presence of plasma is seen to anchor the flame at the nozzle exit, as confirmed in FIGURE 6, which shows representative images of flames with and without plasma for each test case of runs 4, 5 and 6. It resulted that, by increasing the dissipated power, the flame moved from the lift-off condition (test cases 4a, 4b and 4c), to a partial reattachment condition at V_{pp}=10.5 V (test cases 5a, 5b and 5c), before to fully reattach at V_{pp}=16.2 V (test cases 6a, 6b and 6c). Furthermore, as the dissipated power increased, the flame height grew, and the flame appeared more stable, symmetric and well anchored to the nozzle exit. Instead, at fixed applied voltage, the fuel flow rate is seen to have a different impact on the flame of the plasma actuated cases with respect to the clean cases. In absence of plasma actuation, the flame was lifted, and the increase of the fuel flow rate corresponded to a higher lift-off height of the flame up to the blow-off condition. Conversely, when the plasma actuation was enabled, the flame reattached, and the height of plasma assisted flame increased proportionally to the fuel flow rate.

DOI: 10.13009/EUCASS2019-683

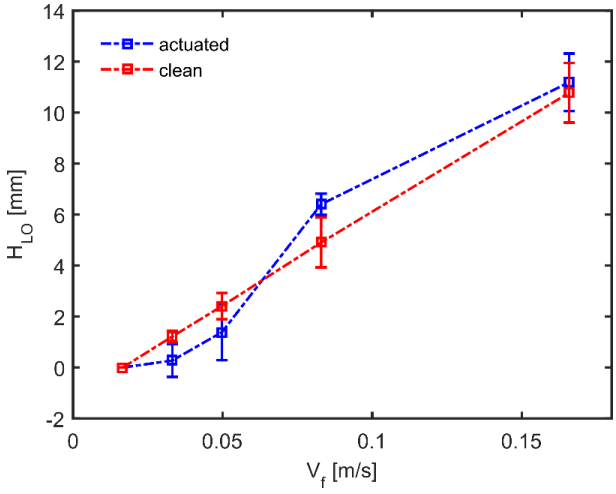

FIGURE 4. The effect of the jet fuel velocity on the flame lift-off height for flames with and without the discharge at a fixed air flow rate equal to 1.54±0.03 g/s.

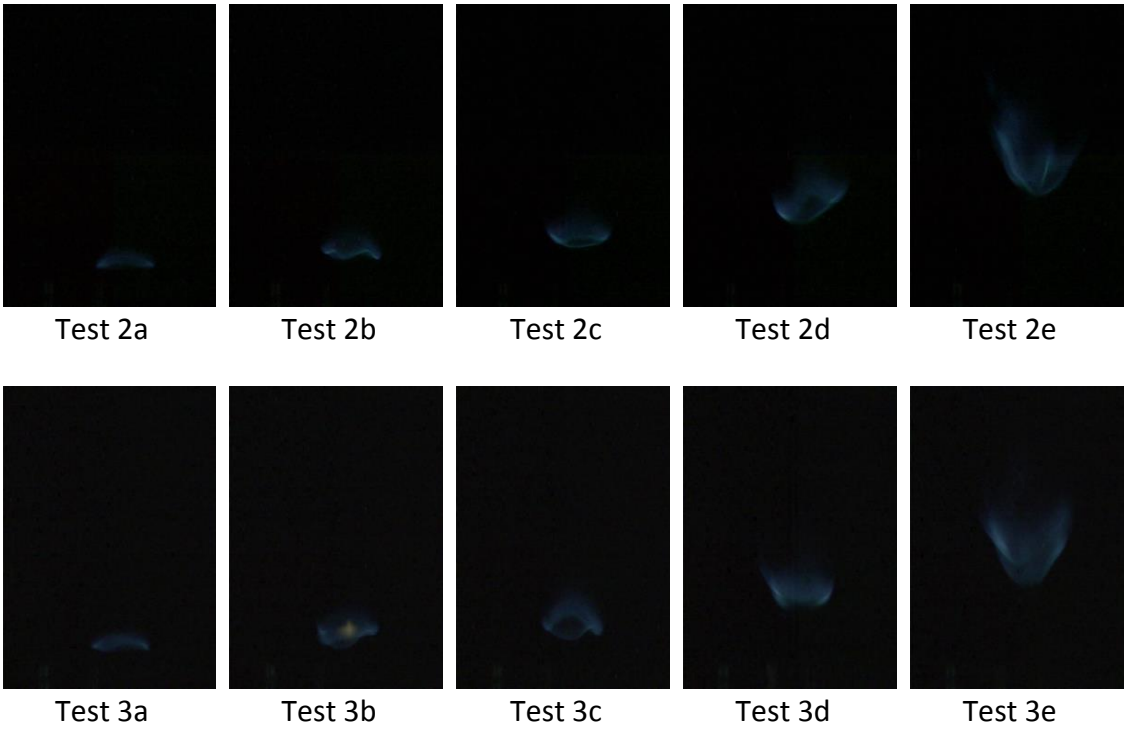

FIGURE 5. Representative instantaneous images of flame without plasma discharges and plasma-attached flames, at different fuel flow rates and fixed air flow rate at 1.54±0.03 g/s.

DOI: 10.13009/EUCASS2019-683

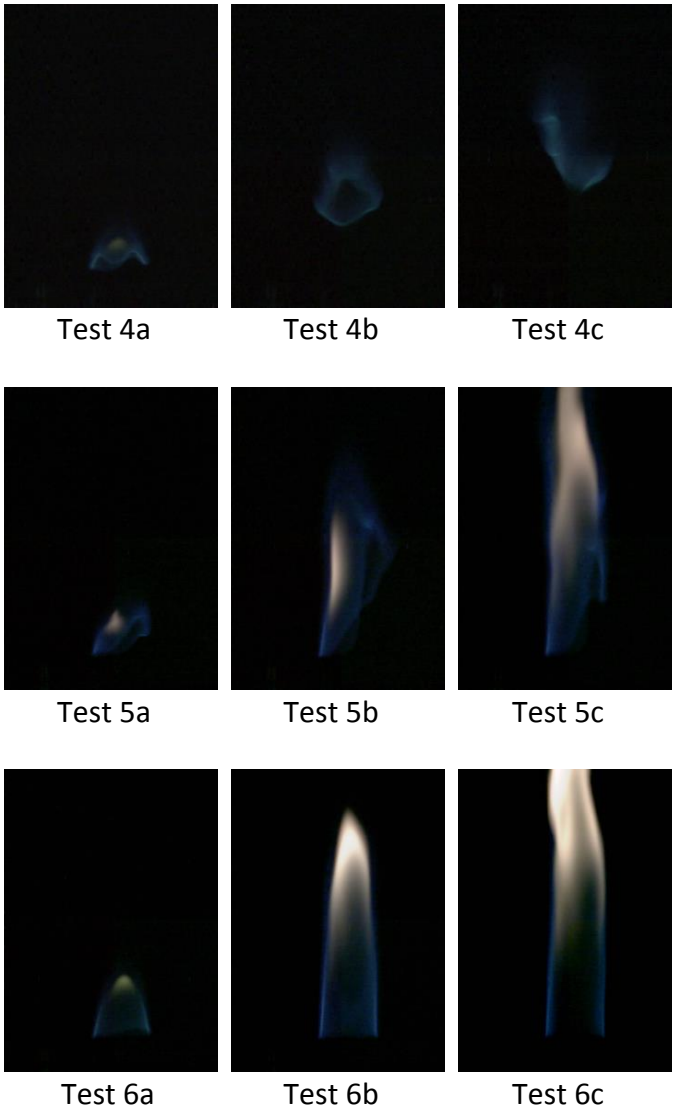

FIGURE 6. Representative instantaneous images of flame without plasma discharges and plasma-attached flames, at different fuel flow rates and fixed air flow rate at 1.35±0.03 g/s.

5. Conclusions

In the present work, an experimental study is carried out to investigate the impact of sinusoidal DBD plasma discharges on the behaviors of lifted non-premixed jet flames fueled with methane. In particular, the effect of a sinusoidal plasma actuation on the flame lift-off distance, length and shape has been experimentally investigated in a Bunsen-type burner with an inner CH_4 jet surrounded by an outer air jet.

Six experimental campaigns have been carried out at several fuel flow rates and plasma power conditions. It was observed that the presence of plasma has an impact on decreasing the lift-off height and altering the flame behaviors. The application of plasma discharges to flame stabilization led to plasma-attached flames or plasma-enhanced lifted flames, depending on the air and fuel flow rates. In particular, at air flow rate of 1.54 g/s, the application of plasma discharges allowed to decrease the lift-off height until the fuel jet velocity was below about 0.05 m/s, thanks to the extension of the flame region upstream toward the burner exit section. Beyond this value, the plasma exhibited no significant impact on the flame lift-off height, even though the amplitude of the lift-off height oscillations reduced, and the lifting flame behavior became more stable. The effect of the plasma actuation improved by reducing the air flow rate. At air flow rate of about 1.35 g/s, plasma-assisted flame reattachment was evident at each fuel velocity, in combination with an increasing flame height proportionally to the fuel jet velocity.

5. Acknowledgement

This work is part of NATO AVT-254.

References

[1] Oh, J., & Noh, D. (2015). Flame characteristics of a non-premixed oxy-fuel jet in a lab-scale furnace. Energy, 81, 328-343. https://doi.org/10.1016/j.energy.2014.12.046.

[2] Lee, S., Padilla, R., Dunn-Rankin, D., Pham, T., & Kwon, O. C. (2015). Extinction limits and structure of counterflow nonpremixed H2O-laden CH4/air flames. Energy, 93, 442-450. https://doi.org/10.1016/j.energy.2015.09.047.

[3] Baigmohammadi, M., Tabejamaat, S., & Zarvandi, J. (2015). Numerical study of the behavior of methane-hydrogen/air pre-mixed flame in a micro reactor equipped with catalytic segmented bluff body. Energy, 85, 117-144. https://doi.org/10.1016/j.energy.2015.03.080.

[4] Gao, X., Duan, F., Lim, S. C., & Yip, M. S. (2013). NOx formation in hydrogen–methane turbulent diffusion flame under the moderate or intense low-oxygen dilution conditions. Energy, 59, 559-569. https://doi.org/10.1016/j.energy.2013.07.022.

[5] Cha, M. S., & Chung, S. H. (1996, January). Characteristics of lifted flames in non-premixed turbulent confined jets. In Symposium (International) on Combustion (Vol. 26, No. 1, pp. 121-128). https://doi.org/10.1016/S0082-0784(96)80208-6.

[6] Chen, Y. C., Chang, C. C., Pan, K. L., & Yang, J. T. (1998). Flame lift-off and stabilization mechanisms of non-premixed jet flames on a bluff-body burner. Combustion and flame, 115(1-2), 51-65. https://doi.org/10.1016/S0010-2180(97)00336-2.

[7] Chung, S. H. (2007). Stabilization, propagation and instability of tribrachial triple flames. Proceedings of the Combustion Institute, 31(1), 877-892. https://doi.org/10.1016/j.proci.2006.08.117

[8] Fokaides, P., & Zarzalis, N. (2007). Lean blowout dynamics of a lifted stabilized, non-premixed swirl flame. In Proceedings of European Combustion Meeting (Vol. 7, p. 2).

[9] Ju, Y., & Sun, W. (2015). Plasma assisted combustion: Dynamics and chemistry. Progress in Energy and Combustion Science, 48, 21-83. https://doi.org/10.1016/j.pecs.2014.12.002.

[10] Pescini, E., De Giorgi, M. G., Francioso, L., Sciolti, A., & Ficarella, A. (2014). Effect of a micro dielectric barrier discharge plasma actuator on quiescent flow. IET Science, Measurement & Technology, 8(3), 135-142. DOI: 10.1049/iet-smt.2013.0131

[11] Kim, Y., Stange, S. M., Rosocha, L. A., & Ferreri, V. W. (2005). Enhancement of propane flame stability by dielectric barrier discharges. Journal of Advanced Oxidation Technologies, 8(2), 188-192. https://doi.org/10.1515/jaots-2005-0210.

[12] Rosocha, L. A., Kim, Y., Anderson, G. K., & Abbate, S. (2007). Combustion enhancement using silent electrical discharges. International Journal of Plasma Environmental Science & Technology, 1(1), 8-13.

[13] Klimov, A., Bityurin, V., Kuznetsov, A., Tolkunov, B., Vystavkin, N., & Vasiliev, M. (2004, January). External and internal plasma-assisted combustion. In 42nd AIAA Aerospace Sciences Meeting and Exhibit (p. 1014). https://doi.org/10.2514/6.2003-698

[14] Bao, A., Utkin, Y. G., Keshav, S., Lou, G., & Adamovich, I. V. (2007). Ignition of ethylene–air and methane–air flows by low-temperature repetitively pulsed nanosecond discharge plasma. IEEE Transactions on Plasma Science, 35(6), 1628-1638. DOI: 10.1109/TPS.2007.910143.

[15] T. Ombrello, S.H. Won, Y. Ju, S. Williams, Flame propagation enhancement by plasma excitation of oxygen. Part I: effects of O 3, Combust. Flame 157 (10) (2010)1906–1915. https://doi.org/10.1016/j.combustflame.2010.02.005.

[16] T. Ombrello, S.H. Won, Y. Ju, S. Williams, Flame propagation enhancement by plasma excitation of oxygen. Part II: effects of O 2 (a 1Δg), Combust. Flame 157(10) (2010) 1916–1928. https://doi.org/10.1016/j.combustflame.2010.02.004.

[17] Starikovskaia, S. M. (2006). Plasma assisted ignition and combustion. Journal of Physics D: Applied Physics, 39(16), R265. https://doi.org/10.1016/j.pecs.2012.05.003.

[18] Kim, Y., Ferreri, V. W., Rosocha, L. A., Anderson, G. K., Abbate, S., & Kim, K. T. (2006). Effect of plasma chemistry on activated propane/air flames. IEEE transactions on plasma science, 34(6), 2532-2536. DOI: 10.1109/TPS.2006.886088.

[19] Pilla, G., Galley, D., Lacoste, D. A., Lacas, F., Veynante, D., & Laux, C. O. (2006). Stabilization of a turbulent premixed flame using a nanosecond repetitively pulsed plasma. IEEE Transactions on Plasma Science, 34(6), 2471-2477. http://dx.doi.org/10.1109/TPS.2006.886081.

[20] Pilla, G. L., Lacoste, D. A., Veynante, D., & Laux, C. O. (2008). Stabilization of a swirled propane–air flame using a nanosecond repetitively pulsed plasma. IEEE transactions on plasma science, 36(4), 940-941. http://dx.doi.org/10.1109/TPS.2008.927343.
[21] Won SH, Cha MS, Park CS, Chung SH. Effect of electric fields on reattachment and propagation speed of tribrachial flames in laminar co-flow jets. Proc Combust Inst 2007; 31:963e70. http://dx.doi.org/10.1016/j.proci.2006.07.166.
[22] Kim, W., Mungal, M. G., & Cappelli, M. A. (2010). The role of in situ reforming in plasma enhanced ultra lean premixed methane/air flames. Combustion and Flame, 157(2), 374-383. DOI: 10.1016/j.combustflame.2009.06.016.
[23] Pescini, E., Francioso, L., De Giorgi, M. G., & Ficarella, A. (2015). Investigation of a micro dielectric barrier discharge plasma actuator for regional aircraft active flow control. IEEE Transactions on Plasma Science, 43(10), 3668-3680. DOI: 10.1109/TPS.2015.2461016.
[24] Pescini, E., De Giorgi, M. G., Francioso, L., Sciolti, A., & Ficarella, A. (2014). Effect of a micro dielectric barrier discharge plasma actuator on quiescent flow. IET Science, Measurement & Technology, 8(3), 135-142. DOI: 10.1049/iet-smt.2013.0131.
[25] Pescini, E., Martínez, D. S., De Giorgi, M. G., & Ficarella, A. (2015). Optimization of micro single dielectric barrier discharge plasma actuator models based on experimental velocity and body force fields. Acta astronautica, 116, 318-332. DOI: 10.1016/j.actaastro.2015.07.015.
[26] Pescini, E., Martinez, D. S., De Giorgi, M. G., & Ficarella, A. (2018). Characterization of the effects of a dielectric barrier discharge plasma actuator on a coaxial jet in a Bunsen burner. Experimental Thermal and Fluid Science, 91, 292-305. https://doi.org/10.1016/j.expthermflusci.2017.10.009.
[27] E. Pescini, D.S. Martínez, M.G. De Giorgi, A. Ficarella, Characterization of the effects of a dielectric barrier discharge plasma actuator on a coaxial jet in a Bunsen burner. Experimental Thermal and Fluid Science, Volume 91, 2018, Pages 292-305, https://doi.org/10.1016/j.expthermflusci.2017.10.009.
[28] Part VI: ANSYS Fluent Magnetohydrodynamics (MHD) module, June 2019, available at https://www.sharcnet.ca/Software/Ansys/17.0/en-us/help/flu_am/flu_mhd.html.